

Effect of interface anisotropy on tilted growth of eutectics:A phase field study

Mei-Rong Jiang(姜美荣), Jun-Jie Li(李俊杰), Zhi-Jun Wang(王志军), and Jin-Cheng Wang(王锦程)
Citation: Chin. Phys. B, 2022, 31 (**10**): 108101. DOI: 10.1088/1674-1056/ac76af
Journal homepage: http://cpb.iphy.ac.cn; http://iopscience.iop.org/cpb

What follows is a list of articles you may be interested in

Multi-phase field simulation of competitive grain growth for directional solidification

Chang-Sheng Zhu(朱昶胜), Zi-Hao Gao(高梓豪), Peng Lei(雷鹏), Li Feng(冯力), and Bo-Rui Zhao(赵博睿)
Chin. Phys. B, 2022, 31 (**6**): 068102. DOI: 10.1088/1674-1056/ac4486

Numerical study of growth competition between twin grains during directional solidification by using multi-phase field method

Chang-Sheng Zhu(朱昶胜), Ting Wang(汪婷), Li Feng(冯力), Peng Lei(雷鹏), and Fang-Lan Ma(马芳兰)
Chin. Phys. B, 2022, 31 (**2**): 028102. DOI: 10.1088/1674-1056/ac0eed

Influence of adatom migration on wrinkling morphologies of AlGaN/GaN micro-pyramids grown by selective MOVPE

Jie Chen(陈杰), Pu-Man Huang(黄溥曼), Xiao-Biao Han(韩小标), Zheng-Zhou Pan(潘郑州), Chang-Ming Zhong(钟昌明), Jie-Zhi Liang(梁捷智), Zhi-Sheng Wu(吴志盛), Yang Liu(刘扬), Bai-Jun Zhang(张佰君)
Chin. Phys. B, 2017, 26 (**6**): 068101. DOI: 10.1088/1674-1056/26/6/068101

Generalized model for laser-induced surface structure in metallic glass

Lin-Mao Ye(叶林茂), Zhen-Wei Wu(武振伟), Kai-Xin Liu(刘凯欣), Xiu-Zhang Tang(汤秀章), Xiang-Ming Xiong (熊向明)
Chin. Phys. B, 2016, 25 (**6**): 068104. DOI: 10.1088/1674-1056/25/6/068104

Migration characterization of Ga and In adatoms on dielectric surface in selective MOVPE

Chen Wei-Jie, Han Xiao-Biao, Lin Jia-Li, Hu Guo-Heng, Liu Ming-Gang, Yang Yi-Bin, Chen Jie, Wu Zhi-Sheng, Liu Yang, Zhang Bai-Jun
Chin. Phys. B, 2015, 24 (**11**): 118101. DOI: 10.1088/1674-1056/24/11/118101

Effect of interface anisotropy on tilted growth of eutectics: A phase field study

Mei-Rong Jiang(姜美荣), Jun-Jie Li(李俊杰), Zhi-Jun Wang(王志军), and Jin-Cheng Wang(王锦程)[†]

State Key Laboratory of Solidification Processing, Northwestern Polytechnical University, Xi'an 710072, *China*

(Received 15 April 2022; revised manuscript received 25 May 2022; accepted manuscript online 8 June 2022)

Interfacial energy anisotropy plays an important role in tilted growth of eutectics. However, previous studies mainly focused on the solid–solid interface energy anisotropy, and whether the solid–liquid interface energy anisotropy can significantly affect the tilted growth of eutectics still remains unclear. In this study, a multi-phase field model is employed to investigate both the effect of solid–liquid interfacial energy anisotropy and the effect of solid–solid interfacial energy anisotropy on tilted growth of eutectics. The findings reveal that both the solid–liquid interfacial energy anisotropy and the solid–solid interfacial energy anisotropy can induce the tilted growth of eutectics. The results also demonstrate that when the rotation angle is within a range of 30°–60°, the growth of tilted eutectics is governed jointly by the solid–solid interfacial energy anisotropy and the solid–liquid interfacial energy anisotropy; otherwise, it is mainly controlled by the solid–solid interfacial energy anisotropy. Further analysis shows that the unequal pinning angle at triple point caused by the adjustment of the force balance results in different solute-diffusion rates on both sides of triple point. This will further induce an asymmetrical concentration distribution along the pulling direction near the solid–liquid interface and the tilted growth of eutectics. Our findings not only shed light on the formation mechanism of tilted eutectics but also provide theoretical guidance for controlling the microstructure evolution during eutectic solidification.

Keywords: tilted eutectics, interfacial energy anisotropy, multi-phase field model

PACS: 81.16.Rf, 81.10.Aj, 81.30.Fb, 81.10.Dn **DOI:** 10.1088/1674-1056/ac76af

1. Introduction

Tilted eutectic,[1–8] in which the growth orientation of eutectics deviates from the direction of the imposed temperature gradient (G) during directional solidification, is a common microstructure for eutectic alloys. As is well known, the mechanical properties of eutectic materials are closely related to its growth orientation. Thus, deep understanding the tilted growth of eutectic is very important for the better control of microstructure and improvement of properties.

Like the tilted growth of dendritic arrays,[9–14] the growth of eutectic is governed by the temperature field, concentration field, and preferred crystal orientation of solidified phase. However, owing to the characteristics of the cooperative growth, the mixed solute diffusion near the front of solid–liquid interfaces, and the force balance at triple points, the tilted growth of eutectic is much more complex than that of dendrite arrays. In particular, typical eutectic patterns are composed of two solid phases with different preferred crystal orientations, which makes the tilted growth of eutectic more flexible and thus more complex in turn.

Up to now, many efforts have been made to elucidate the formation of tilted eutectics. Several experimental and theoretical studies[3,4,6,15–21] suggested that the tilted growth of eutectic lamellae is dependent on the solidification dynamic behavior. It was well demonstrated that the solidification dynamic behavior often relies on initial conditions,[22,23] in which the initial lamellae spacing λ_0 is an important factor that influences the dynamics behavior. When $\lambda_0 > a\lambda_m$, where a is a constant related to the solidification conditions and λ_m is the minimum undercooling spacing,[24] a homogeneous tilt bifurcation (a tilted periodic state) was observed.[6] And a parity-breaking transition from the symmetric state to a tilted state has also been observed for the liquid–solid interface front profile during the tilted growth of eutectics.[19] Although these reports presented some explanations on the formation of tilted eutectics, the effect of the anisotropic interface energy on tilted growth of eutectics was not taken into account.

With the development of eutectic solidification theory and research methods, the importance of interfacial energy anisotropy on tilted eutectics is well recognized.[7,25–34] From the *in-situ* directional solidification experiments of transparent alloys, Caroli *et al.*[25] found that the tilted growth of lamellae and symmetry reflection of the solid–liquid interface front profile are broken, induced by interfacial energy anisotropies. Having made further theoretical analysis, they concluded that the anisotropy of solid–solid interface energy attempts to tilt lamellae into the orientation with the lowest α/β interface energy, while the anisotropy of solid–liquid interface energy may modify the pinning angle for α phase and β phase at triple points. Thus, it can be assumed that the contribution of solid–solid interface energy anisotropy to eutectic growth is comparable to that of solid–liquid interface energy anisotropy. Akamatsu *et al.*[7] observed that the shape of solid–liquid interface

[†]Corresponding author. E-mail: jchwang@nwpu.edu.cn

© 2022 Chinese Physical Society and IOP Publishing Ltd

in anisotropy-driven traveling lamellae patterns can be maintained to be approximately mirrorsymmetric by a modified directional solidification methodology called rotating directional solidification. To simplify the analysis, they further assumed that the shape of the solid–liquid interface is exactly symmetric; in other words, they omitted the effect of solid–liquid interface energy anisotropy on the formation of eutectics and concluded that the solid–solid interface anisotropy plays an important role in the forming of tilted eutectics. Based on Akamatsu *et al.*'s experimental results, Ghosh *et al.*[35–37] investigated the effect of solid–solid interface energy anisotropy on tilted growth of eutectics by using a multi-phase field model, and found that the anisotropy of solid–solid interphase energy can significantly affect the growth direction of eutectics. Tu *et al.*[38,39] further investigated the effect of solid–solid interphase energy anisotropy on lamellar eutectic morphology. They found that when λ_0 is slightly larger than λ_m, the lamellar morphology is mainly affected by the anisotropic interface energy of two solid phases, which results in the formation of a stable tilted lamellar pattern. However, when λ_0 is significantly larger than λ_m, the morphology is controlled by the variation of λ_0, resulting in the formation of an unstable mixed oscillation pattern.

In summary, the investigations mentioned above[7,25–39] have demonstrated that the anisotropic interface energy plays a vital role in the forming of tilted eutectics. However, the effect of the solid–liquid interface energy anisotropy on the tilted growth of eutectics is often ignored. As mentioned earlier by Caroli *et al.*,[25] the effect of solid–liquid interface energy anisotropy on the pinning angle for α phase and β phase at triple points during eutectic solidification have been confirmed. As is well known, a small variation of the pinning angle can significantly influence the local force balance at triple points, which will sharply influence microstructure evolution. Thus, further investigations of the effect of solid–liquid interface energy anisotropy on the formation of tilted eutectics are urgently needed. And the mutual interaction between the anisotropic solid–solid interface energy and the solid–liquid interfaces energy is also a challenge.

The phase field method, as a popular mesoscale numerical method, has been demonstrated as a powerful method in investigating microstructure evolution. Especially, the multiphase field model has been employed widely to study the eutectic solidification.[40–43] In this study, a multiphase field model was employed to investigate the effect and mechanism of solid–liquid interface energy anisotropy on tilted eutectics. Moreover, the interactions between solid–solid and solid–liquid interface energy anisotropy during the formation of tilted eutectics are also explored.

2. Methods

2.1. Phase field model

In binary eutectic solidification, two solid phases (α and β) are simultaneously formed from the melt (L). Thus, the multi-phase field model proposed by Kim *et al.*[40,44] was employed to study the tilted growth of eutectics in this study. Three order parameters ϕ_i $(i=1,2,3)$ were introduced to distinguish different phases during eutectic solidification: $\phi_1=1$, $\phi_2=0$, $\phi_3=0$ represents the liquid phase, $\phi_1=0$, $\phi_2=1$, $\phi_3=0$ and $\phi_1=0$, $\phi_2=0$, $\phi_3=1$ denote the bulk phase of α and β, respectively. And $0<\phi_i$ $(i=1,2,3)<1$ indicates the interface.

A general free energy function description in this multiphase field model of a eutectic system includes the interfacial free energy f^{P} and thermodynamic potential f^{T}, which can be written as

$$F=\int\left[f^{\mathrm{P}}+f^{\mathrm{T}}+\xi\left(\sum_i\phi_i-1\right)\right]\mathrm{d}V, \tag{1}$$

where ξ is the Lagrange multiplier for the restriction condition conserving the sum of phase fields at random point in the system. According to the variational principle, the governing equation of the phase-field variable can be described as

$$\frac{\partial\phi}{\partial t}=-\frac{2}{N}\sum_{j\neq i}^{3}s_{ij}M_{ij}\left[\frac{\delta F}{\delta\phi_i}-\frac{\delta F}{\delta\phi_j}\right]. \tag{2}$$

Here, $s_{ij}=s_is_j$ is a step function. If $\phi_i>0$, $s_i=1$; otherwise $s_i=0$. M_{ij} is the phase field mobility across the i/j interface.

The governing equation of the diffusion field can be written as

$$\frac{\partial c}{\partial t}=\nabla\cdot D\sum_i^3\phi_i\nabla c_i, \tag{3}$$

where D is the solute diffusivity.

A linear temperature approximation is used to describe the temperature field evolution during directional solidification, which can be written as

$$\frac{\partial T}{\partial t}=\frac{\partial(T_0+G(x-Vt))}{\partial t}=-GV, \tag{4}$$

where T_0 is the initial solidification temperature, G is the temperature gradient, and V is the pulling velocity.

2.2. Interfacial energy anisotropy

A two-fold symmetric interfacial energy anisotropy function[35–37] was used to characterize the effect of interfacial energy anisotropy on the formation of tilted eutectics. It can be expressed as

$$\gamma=\gamma_0\left(1-\delta\cos 2\left(\theta-\theta_{\mathrm{R}}\right)\right), \tag{5}$$

where γ denotes the interface energy; γ_0 the average interface energy; δ the anisotropy strength: δ is set to be 0.005 when interface energy is anisotropic, and 0.0 when interface energy is isotropic; θ_{R} is the rotation angle, which is defined as the angle

between the preferred crystal axis and the direction of G; θ is the angle between the interface normal direction and the x axis as shown in Fig. 1(a). Figure 1(b) shows the schematic definitions of simulation parameters used in the prensent study, where the y axis is parallel to the G. The tilt angle (θ_t) is the angle between the direction of the lamellae growth and that of the G direction. Here, the direction, from the center position of the bulk phase (α or β) at the beginning of solidification to that at the ending of solidification, is defined as the eutectic growth direction. Thus, θ_t can be easily measured as shown in Fig. 2(a). The other parameters in Fig. 1(b) will be described in Section 3.

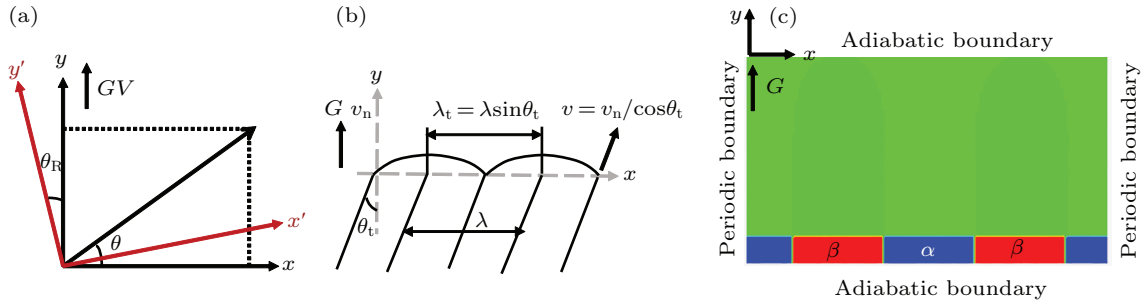


Fig. 1. (a) Definition of θ and θ_R, (b) definitions of θ_t, (c) initial eutectic patterns and boundary conditions.

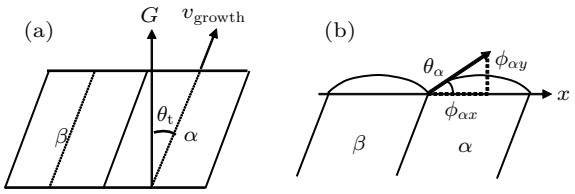


Fig. 2. Schematics of measurement of (a) tilt angle and (b) pinning angle.

2.3. Parameters

In this study, we took a binary eutectic alloy with a symmetric phase diagram[36] for example, and all parameters used in this simulation are listed in Table 1.

Table 1. Parameters used in this simulation.

Parameters, (symbols)	Unit	Values
Eutectic temperature, T_e	K	360.0
Eutectic concentration, c_e	Mol%	0.5
Liquids slope of α, $m_{L/\alpha}$	K/(at.%)	−80.0
Liquids slope of β, $m_{L/\beta}$	K/(at.%)	80.0
Partition coefficient of α, k_α	–	0.5
Partition coefficient of β, k_β	–	1.5
Interfacial energy, $\gamma_{L/\alpha}$	J/m^2	6.0×10^{-3}
Interfacial energy, $\gamma_{L/\beta}$	J/m^2	6.0×10^{-3}
Interfacial energy, $\gamma_{\alpha/\beta}$	J/m^2	12.0×10^{-3}
Diffusivity in liquid, D_L	J/m^2	5.0×10^{-10}
Diffusivity in α and β, D_s	m^2/s	5.0×10^{-14}
Temperature gradient, G	K/m	8.0×10^{3}
Pulling velocity, V	m/s	2.0×10^{-6}
Grid, dx	m	1.5×10^{-6}
Time step, dt	s	1.8×10^{-5}

All simulations were performed in a domain of $800\,\mathrm{d}x \times 100\,\mathrm{d}x$ with a regular grid. The initial eutectic patterns were set to be a periodic lamellae with a size of $10\,\mathrm{d}x \times 100\,\mathrm{d}x$ at the bottom of the simulation cell and paralleled to the G. Periodic boundary conditions were imposed in the x-axis direction, indicating an infinite periodic cycle of lamellae along the x axis, while adiabatic boundary conditions were used in the y direction to ensure the solute conservation in this direction[40] as shown in Fig. 1(c).

3. Results and discussion

3.1. Effect of interface energy anisotropy on tilted growth of eutectics

Figure 3 shows the evolution of eutectic morphologies under different interface energy conditions and $\theta_R = 45°$. The triple-point trajectories and the local force balance at the triple points, are also presented. From this figure, one can see that the lamellar growth direction aligns with the direction of G when interface energy is isotropic. The pinning angle for α phase and β phase at the triple points are the same, *i.e.*, $\theta_\alpha(61°) = \theta_\beta(61°)$. Here, the pinning angle is defined as the angle between the tangent of the solid–liquid interface and the x axis at triple points. It can be determined from two steps: firstly calculating the value of ϕ_y/ϕ_x; and then determining the pinning angle from the arctan function $\theta_\alpha = \arctan(\phi_{\alpha y}/\phi_{\alpha x})$, and the results are shown in Fig. 2(b). The same pinning angles at triple points indicate that the solid–liquid interface of L/α and L/β are symmetrical. Component force of L/α interfacial tension ($\sigma_{L\alpha}$) and L/β interfacial tension ($\sigma_{L\beta}$) in the x-axis direction are equal, resulting in that the minimum interfacial tension of solid–solid interface is parallel to the direction of G (y axis). As is well known, during eutectic solidification, the lamellar growth direction always coincides with the direction of the minimum solid–solid interfacial tension. Therefore, the direction of eutectics growth aligns with that of G, that is, non-tilted growth of lamellae occurs as shown in Fig. 3(a). However, when interface energy is anisotropic, the lamellar growth direction deviates from the direction of G clearly. This indicates that the interface energy anisotropy has a significant effect on the lamellar growth direction. Generally,

during eutectic solidification, when there exists anisotropic interface energy, the growth rates for different crystal planes are not the same, and the plane with a small interface energy will grow slow. The plane that grows fast will disappear, while the plane that grows slow is preserved in the crystal growth process. The difference in growth rate between different planes will induce the misalignment between the direction of minimum solid–solid interfacial tension and that of G. Consequently, the tilted growth of lamellae is observed as shown in Figs. 3(b)–3(d). And the force balance at triple points is shown at the bottom of Fig. 3, where the dashed vectors represent the isotropic force vectors, the solid vectors are the anisotropic ones, and $\theta_{\alpha 1}$, $\theta_{\beta 1}$ denote the deviation between the isotropic force vectors and the anisotropic ones. When L/α interface energy is anisotropic, the force vector in the case of with anisotropy (the red solid arrow at the bottom of Fig. 3(b)) is different from that of without anisotropy (the red dashed arrow at the bottom of Fig. 3(b)). This variation of force vector $\boldsymbol{\sigma}_{L/\alpha}$ will induce variations of other vectors ($\boldsymbol{\sigma}_{L/\beta}$, $\boldsymbol{\sigma}_{\alpha/\beta}$) at triple points to maintain the force balance, resulting in the direction misalignment between the minimum solid–solid interfacial tension and G as shown at the bottom of Fig. 3(b). Similar processes are also observed when L/β or β/α interface energy is anisotropic as shown by the force balance at bottom of Figs. 3(c) and 3(d), respectively. Moreover, it is found that the pinning angles for α phase and β phase at the triple points obviously are not the same even when θ_t is small. This reveals that the symmetry of solid–liquid interface front profile is broken spontaneously when eutectic lamellae grows obliquely. However, noticeable discrepancies appear in θ_t under different interfacial energy anisotropy conditions. From Figs. 3(b) and 3(c), it can be seen clearly that θ_t (1.4°) caused by L/α interface energy anisotropy is smaller than that (6.4°) caused by L/β interface energy anisotropy. This is because of different concentration distributions at the front of L/α and L/β, which induces different driving forces in the cases of α and β. From Figs. 3(c) and 3(d), it can be observed that θ_t (1.1°) caused by α/β interface energy anisotropy is smaller than that (6.4°) caused by L/β interface energy anisotropy. The reason for this phenomenon is that the direction deviation between the preferred orientation of β and the direction of G induces the anisotropy of the L/β interface energy, whereas the difference in the relative crystal orientation between α direction and β direction induces the anisotropy of the α/β interface energy.

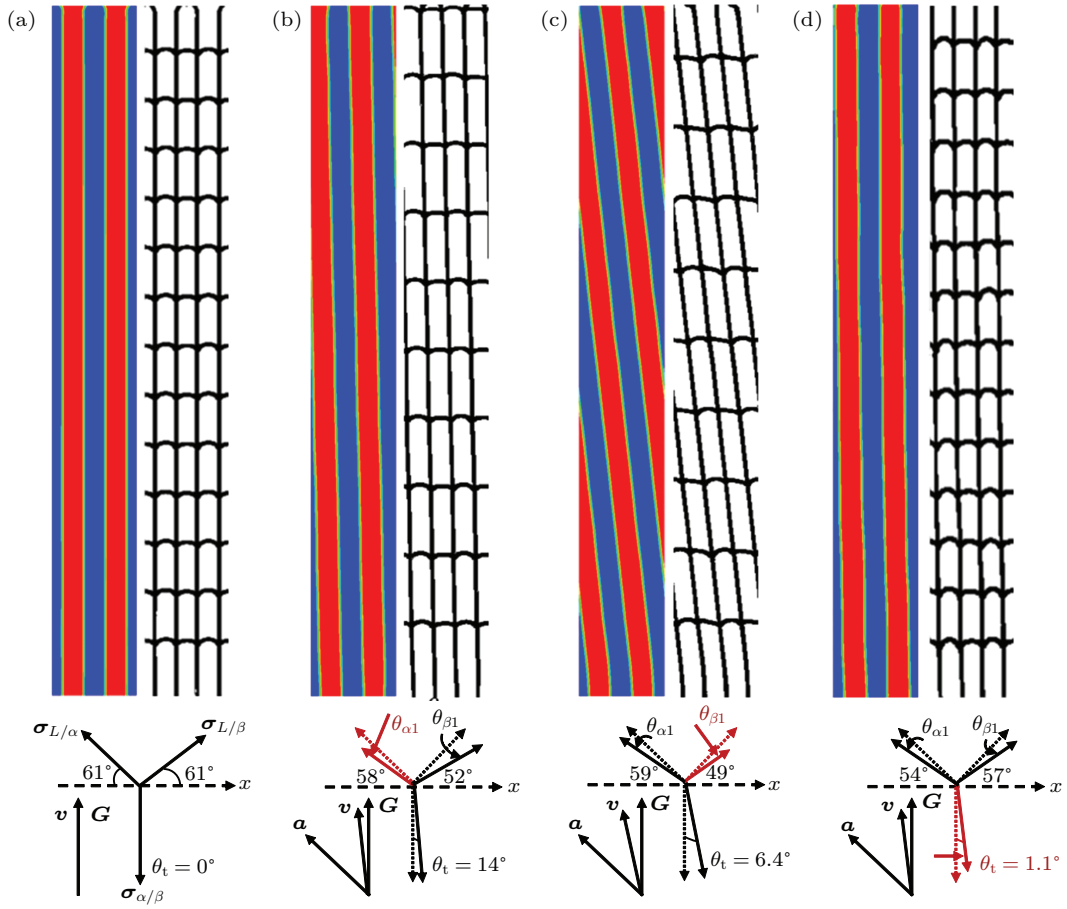


Fig. 3. Lamellar patterns, interface trajectories, and local force balance at triple points under different interfacial energy conditions, where $\boldsymbol{a}$ indicates preferred crystal orientation and v is growth rate of lamellae, showing (a) isotropic interface energy, (b) L/α interface energy anisotropy, (c) L/β interface energy anisotropy, and (d) α/β interphase energy anisotropy.

Figure 4 shows the curve of θ_t *versus* θ_R under different conditions of interfacial energy anisotropies. It is obvious that the whole trend of variation of θ_t with θ_R is almost the same when the interface energy is anisotropic, *i.e.* θ_t increases initially and then decreases with the increase of θ_R. However, obvious difference in variation trend between different anisotropic interface energy are also observed. When the solid–liquid (L/α, or L/β, or L/α and L/β) interface energy is anisotropic and θ_R is small, a very small θ_t is observed. The preferred lamellae orientation deviates slightly from the direction of G, resulting in small variations of the pinning angle for both α phase and β phase at triple points. These small variations of the pining angle further result in a small deviation of the direction of minimum solid–solid interfacial tension from the direction of G. On the contrary, a large θ_t is observed when α/β interface energy is anisotropic and θ_R is small. In this case, the relative difference in crystal orientation between two solid phases is small. However, the preferred orientation direction of α ($\boldsymbol{a}_\alpha$) and β ($\boldsymbol{a}_\beta$) are the same, *i.e.*, all the preferred orientations are leftward as shown in Fig. 5(a), indicating that $\boldsymbol{a}_\alpha$ and $\boldsymbol{a}_\beta$ can promote the tilted growth of lamellae. With the increase of θ_R, θ_t increases gradually, whether there exists interface energy anisotropy of solid–liquid or that of solid–solid, but the trend of its increase with solid–liquid interface energy anisotropy is obviously slower than with solid–solid interface energy anisotropy. When θ_R is large and solid–liquid interface energy is anisotropic, a large θ_t is found. The preferred orientation of lamellae greatly deviates from the direction of G, resulting in large variations of pinning angle for α phase and β phase at triple points, thus inducing a large θ_t by maintaining the local force balance. In contrast, a small θ_t is observed when solid–solid interface energy is anisotropic and θ_R is large. The relative difference in crystal orientation between α and β is very large. If the preferred orientation of α ($\boldsymbol{a}_\alpha$) remains unchanged, the direction of $\boldsymbol{a}_\beta$ changes from left to right, and the preferred orientation of $\boldsymbol{a}_\alpha$ and $\boldsymbol{a}_\beta$ are opposite as shown in Fig. 5(b). Owing to the coupled growth of the two eutectic phases during solidification, the growth direction of eutectics tends to be parallel to the direction of G. Similarly, when θ_R is very large, θ_t is very small or even nearly 0°, with a solid–solid interface energy anisotropic. Whereas, when the solid–liquid interface energy is anisotropic and θ_R is very large, the preferred orientation of lamellae trends to be perpendicular to the direction of G. Theoretically, θ_t should be very large, but large θ_t must match large $\theta_{\alpha 1}$ and $\theta_{\beta 1}$ to keep the force balance at triple points. It is a common fact that large angle variation needs larger energy than small one at triple point. If the θ_t is very large, the stable state cannot be obtained easily during solidification. Thus, θ_t will decrease with θ_R increasing further after achieving the maximum tilt angle.

In addition, a θ_R corresponding to the maximum tilt angle of lamellae (θ_{t_max}) is observed from Fig. 4. However, obvious discrepancies of the θ_R corresponding to the θ_{t_max} under different conditions of interfacial energy anisotropy are found. From Fig. 4(a), one can see that the θ_R corresponding to the θ_{t_max}, with L/α interface energy anisotropic, is approximately 60°; while that, with L/β interface energy anisotropic, is approximately 50°. When both L/α interface energy and L/β interface energy are anisotropic, the θ_R corresponding to the θ_{t_max} is approximately 60°. This suggests that difference in anisotropy of the solid–liquid interface energy may result in the difference in tilted growth through the adjustment of the force balance at triple points. As clearly shown in Fig. 4(b), the θ_R corresponding to the θ_{t_max}, with both L/α and L/β interface energy anisotropic, is approximately 60°, whereas that, with the α/β interface energy anisotropic, is approximately 20°. This indicates that the effect of energy anisotropy of solid–liquid interface and solid–solid interface on tilted eutectics are different, and the θ_{t_max} is related to θ_R.

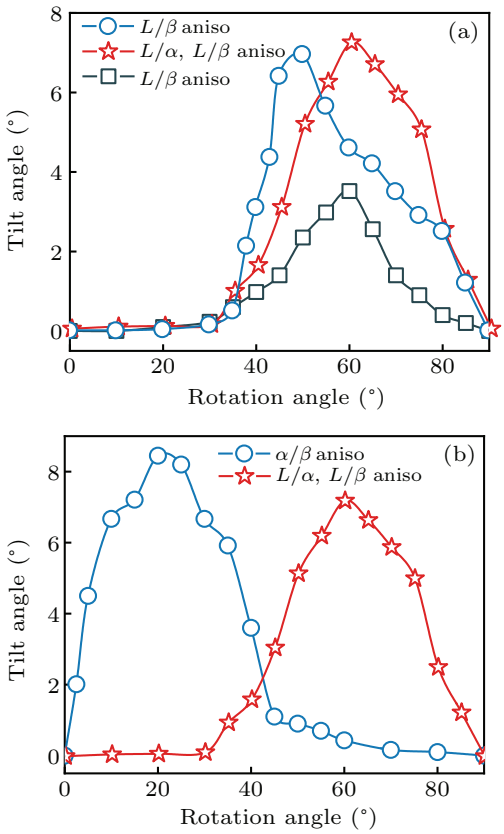


Fig. 4. (a) Curves of θ_R *versus* θ_t with different solid–liquid (L/α, L/β, or L/α and L/β) interface energy anisotropy (aniso), and (b) curves of θ_R *versus* θ_t with solid–liquid (L/α and L/β) interface energy anisotropy and α/β interface energy anisotropy.

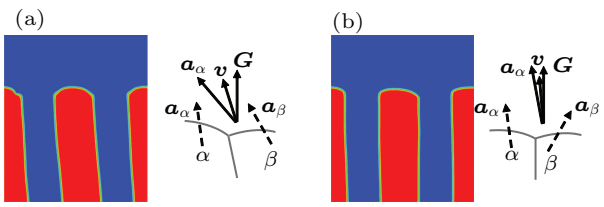


Fig. 5. Phase-field patterns and schematics of crystal orientation of two-solid phases with different rotation angles: (a) $\theta_R = 10°$ and (b) $\theta_R = 60°$.

3.2. Tilted growth with both anisotropies of solid–liquid and solid–solid interface energy

Figure 6 shows the eutectic patterns against rotation angle when both L/α, L/β, and α/β interface energies are anisotropic. It can be found that as θ_R increases, the growth direction of eutectic lamellae gradually deviates from the direction of G, *i.e.*, θ_t increases gradually. However, with the further increase of θ_R, the growth of lamellae changes from tilted to non-tilted growth. In addition, when $\theta_R = 20^\circ$, the solid–solid interphase is rough, *i.e.*, a small disturbance appears. Through the stable growth rate of lamellae and concentration distribution at the front of the solid–liquid interface, it is demonstrated that this disturbance of the solid–solid interphase is not induced by the instable growth of eutectic. Thus, a conclusion can be obtained that anisotropic interface energy may induce a non-smooth solid–solid interface. This may result from a small adjustment of interlamellar spacing caused by the anisotropic force balance at triple point.

Figure 7 shows the comparison between the simulated and the measured curves of θ_R *versus* θ_t. It can be seen that when L/α, L/β, and α/β interface energies are anisotropic, the θ_R corresponding to the θ_{t_max} from phase field simulations is approximately 30°, which accord well with the experimental results by Akamatsu *et al.*[7] However, the θ_R corresponding to the θ_{t_max} is 20° when only α/β interface energy is anisotropic, whereas it is 60° when both L/α and L/β interface energies are anisotropic. This reveals that the solid–liquid (L/α, L/β) and solid–solid (α/β) play vital roles in the forming of tilted eutectics. Moreover, when L/α, L/β, and α/β interface energies are anisotropic and θ_R is larger than 60°, θ_t is small, which is the same as the case of α/β interface energy anisotropy, indicating that the solid–solid interfacial energy anisotropy plays an important role in the tilted growth of lamellae, while the anisotropy of solid–liquid interface energy plays a less important role. However, the latter anisotropies can still influence the θ_R corresponding to the θ_{t_max} by affecting the local force balance at triple point. When L/α, L/β, and α/β are anisotropic and θ_R is small (less than 30°), a large θ_t appears. This is also similar to the case of α/β interface energy anisotropy, suggesting that the tilted growth of lamellae is mainly controlled by the anisotropy of α/β interface energy. However, when θ_R is approximately 40°, and L/α, L/β, and α/β interface energies are anisotropic, θ_t can be regarded as the superposition of contributions from the solid–liquid solid–solid interface energy anisotropy and the solid–solid interface energy anisotropy. This indicates that the tilted growth of lamellae is affected not only by solid–solid interface energy anisotropy, but also by solid–liquid interface energy anisotropy.

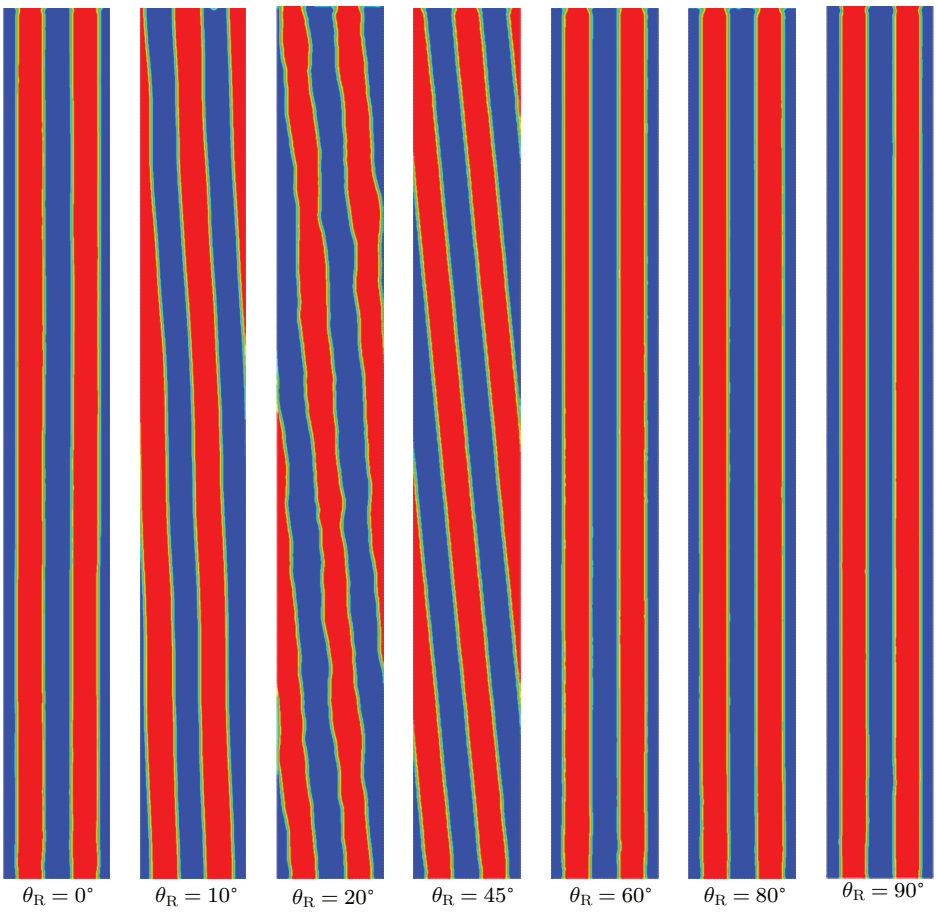


Fig. 6. Variation of lamellar patterns with rotation angle with interface energy being anisotropic for all interfaces (L/α, L/β, and α/β).

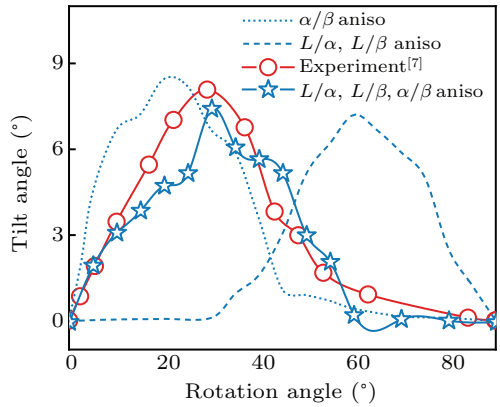


Fig. 7. Comparison between simulated and measured curves of tilt angle (θ_t) *versus* rotation angle (θ_R) for different interface energy anisotropies.

As is well known, the distributions of solute concentration near the front of solid–liquid interface greatly influence the microstructural evolution during solidification. To further explore the effect of anisotropic interface energy on the formation of tilted eutectic, the solute concentration distribution at the front of the solid–liquid interfaces are investigated. Studies[7,25] have shown that the concurrent or competitive contributions of the anisotropies of solid–liquid interface energy and solid–solid one on the formation of eutectic patterns may exist. This implies that the local force balance at triple point is highly complex when interface energy is anisotropic. However, the force balance at the triple point must be maintained during the eutectic solidification, *i.e.* the following equations need to be satisfied:

$$\begin{cases} \boldsymbol{\sigma}_{\alpha\beta}\sin\theta_t + \boldsymbol{\sigma}_{L\alpha}\cos\theta_\alpha = \boldsymbol{\sigma}_{L\beta}\cos\theta_\beta, \\ \boldsymbol{\sigma}_{L\alpha}\sin\theta_\alpha + \boldsymbol{\sigma}_{L\beta}\sin\theta_\beta = \boldsymbol{\sigma}_{\alpha\beta}\cos\theta_t. \end{cases} \tag{6}$$

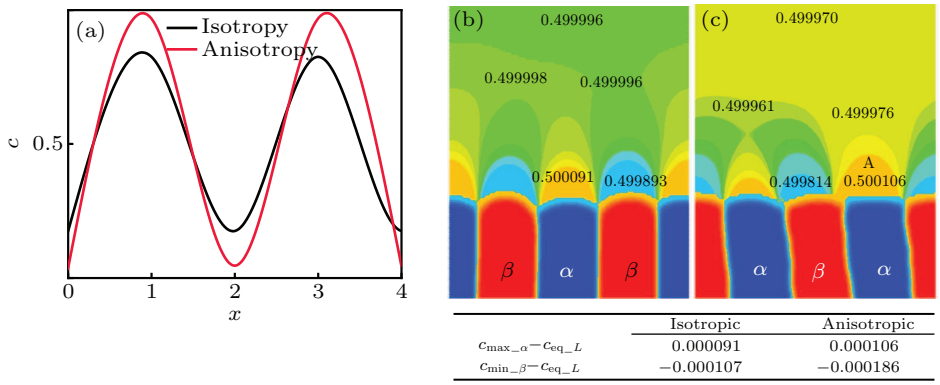
When interface energy is isotropic ($|\boldsymbol{\sigma}_{L\alpha}| = |\boldsymbol{\sigma}_{L\beta}|$), the pinning angle of α (θ_α) equals that of β (θ_β) at triple points. According to Eq. (6), it can be obtained easily that θ_t equals 0°, indicating that the component forces $\boldsymbol{\sigma}_{L\alpha}$ and $\boldsymbol{\sigma}_{L\beta}$ in the x direction can be canceled out. And non-tilted growth of lamellae is observed. However, when interface energy is anisotropic, the pinning angle $\theta_\alpha \neq \theta_\beta$ at triple point, indicating that θ_t must not be equal to 0°, and the component forces $\boldsymbol{\sigma}_{L\alpha}$ and $\boldsymbol{\sigma}_{L\beta}$ in the x direction are not canceled out. Thus, there must be a force in the x-axis direction that drives the evolution of eutectic patterns, resulting in the tilted growth of lamellae. When eutectic patterns grow obliquely, the growth rate can be expressed as $v = v_n/\cos\theta_t$, and the interlamellar spacing $\lambda = \lambda_t/\sin\theta_t$, where v_n is the normal growth rate of lamellae, and λ_t is the tangential interlamellar spacing as shown in Fig. 1(b). Therefore, if the interface energy is anisotropic, the solution of the solute diffusion equation at the front of the interface is as follows:

$$\begin{aligned} c &= c_e + c_\infty + B_0 \exp\left(-\frac{v\cos\theta_t}{D}\right) \\ &\quad + \sum_{n=1}^{\infty} B_n \cos\left(\frac{2n\pi x}{\lambda\sin\theta_t}\right)\exp\left(-\frac{2n\pi y}{\lambda\sin\theta_t}\right), \end{aligned} \tag{7}$$

$$\begin{aligned} B_0 &= \frac{2(c_0^\alpha\lambda_\alpha - c_0^\beta\lambda_\beta)}{\lambda}, \\ B_n &= \frac{\lambda\sin\theta_t v\cos\theta_t c_0}{(n\pi)^2 D}\sin\left(\frac{2n\pi\lambda_\alpha}{\lambda}\right), \end{aligned} \tag{8}$$

where c_∞ is the actual composition far from the solid–liquid interface during eutectic solidification and λ_i is the half-width of the i phase. According to Eq. (7), the solute distributions at the front of the solid–liquid interface for the tilted (anisotropic interface energy) and non-tilted growth of lamellae (isotropic interface energy) are shown in Fig. 8(a). It can be observed that the concentration gradients at the front of the interface with interfacial energy anisotropy are higher than without interfacial energy anisotropy. This indicates that the concentration disturbance near the solid–liquid interface with anisotropic interface energy is larger than without anisotropic interface energy. It should also be noted that no solution can be obtained from Eq. (7) if the tilt angle of lamellar is 0° and interface energy is anisotropic. However, in this case, the solution still exists, which is because only very small variation of pinning angle at triple point occurs to keep the force balance. The small variation will further induce different solute-diffusion rates on both sides of triple point, leading to a large concentration disturbance near the solid–liquid interface. Although this concentration disturbance is not enough to induce the tilted growth of eutectics, it can result in a larger concentration gradient at the front of the solid–liquid interface than the counterpart of isotropic interface energy. Thus, the same conclusion still holds true even when the tilt angle of lamellar is 0° and interface energy is anisotropic. Figures 8(b) and 8(c) show the solute concentration distributions near the solid–liquid interfaces obtained by phase-field simulations with and without anisotropic interface energy, respectively. The differences between the maximum solute concentrations of α ($c_{\min_\alpha}$) at the front of the solid–liquid interface and the equilibrium concentrations in the liquid (c_{eq_L}) with and without anisotropic interface energy are shown in the lower right of Fig. 8. The differences between the minimum solute concentrations of β ($c_{\min_\beta}$) at the front of the solid–liquid interface and c_{eq_L} with and without anisotropic interface energy are also shown in the lower right of Fig. 8. It can be clearly seen that the concentration gradient from phase-field simulation near the solid–liquid interface with isotropic interface energy is lower than with anisotropic one. This result is in good agreement with the theoretical solution of the solute diffusion equation, demonstrating the reliability of our phase field results. Moreover, when the interface energy is isotropic, the solute concentration distribution at the front of the solid–liquid interface is almost symmetrical along the y axis. However, when the interface energy is anisotropic, it is almost symmetrical along the inclined growth axis. This symmetrical concentration distribution along the inclined growth axis is because different

pinning angles at triple point will result in different solute diffusion rates on both sides of triple point. In addition, owing to the G and V existing along the y direction, the symmetrical axis of solute concentration distribution near the solid–liquid interface that tends to be parallel to the direction of G may be observed as shown at point A of Fig. 8(c). Theoretically, this solute distribution near point A of Fig. 8(c) cannot maintain stable tilted growth of lamellae. However, if the strength of interface energy anisotropy is sufficiently high, the effect of G on solute concentration distribution is lower than that of anisotropic interface energy. The effect of concentration distribution near point A of Fig. 8(c) on the tilted growth of the lamellae can be ignored. Consequently, the stable tilted growth of lamellae can be obtained.



	Isotropic	Anisotropic
$c_{\max_\alpha} - c_{\mathrm{eq}_L}$	0.000091	0.000106
$c_{\min_\beta} - c_{\mathrm{eq}_L}$	−0.000107	−0.000186

Fig. 8. Concentration distributions near the interfaces: (a) theoretical prediction results with isotropic and anisotropic interface energies, respectively, (b) phase-field simulation results with isotropic interface energy, and (c) phase-field simulation results with L/α, L/β, and α/β interface energy anisotropies.

It should also be noted that beside the interface energy anisotropy, the initial conditions, such as initial lamellar spacing, is also an important factor on the tilted growth of eutectics. In this study, however, we restrict ourselves to a range of regular lamellar eutectic formed by the initial lamellar spacing to investigate the effect of interfacial energy anisotropy on tilted growth of eutectic. As to the case of irregular eutectic structures, *i.e.*, the initial lamellar spacing is beyond this range, so, further studies are needed.

4. Conclusions

Based on the multi-phase field model, the effect of solid–liquid or solid–solid energy anisotropy on the tilted growth of lamellae during eutectic solidification is investigated. And the mutual interactions between solid–liquid and solid–solid interface energy anisotropies are explored. The results show that both the solid–liquid and solid–solid interface energy anisotropies can induce the tilted growth of lamellae. When the anisotropy of solid–solid interface energy and solid–liquid interface energy are considered, the phase-field simulation results are in good agreement with the experimental results, indicating that the anisotropies of solid–solid and solid–liquid interface energies play important roles in tilted growth of eutectic. However, when θ_{R} is small (less than 30°) or large (higher than 60°), the tilted growth of eutectic patterns is mainly controlled by the solid–solid interface energy anisotropy; whereas if θ_{R} is between 30° and 60°, and the tilted growth is jointly affected by both solid–liquid interface energy anisotropy and solid–solid interface energy anisotropy. In addition, the results also demonstrate that the solute concentration gradient with anisotropic interface energy is higher than with isotropic interface energy, which is in good agreement with the theoretical analysis of the solute diffusion equation. Our findings not only elucidate the formation mechanism of tilted eutectics but also provide theoretical guidance for controlling the microstructure evolution.

Acknowledgements

The authors thank the High-Performance Computing Center of Northwestern Polytechnical University, China, for the computer time and facilities.

Project supported by the National Natural Science Foundation of China (Grant Nos. 51871183 and 51571165).

References

[1] Double D D, Truelove P and Hellawell A 1968 *J. Cryst. Growth* **2** 191
[2] Cline H E 1981 *J. Appl. Phys.* **52** 256
[3] Faivre G and Mergy J 1992 *Phys. Rev. A* **46** 963
[4] Faivre G and Mergy J 1992 *Phys. Rev. A* **45** 7320
[5] Mergy J, Faivre G, Guthmann C and Mellet R 1993 *J. Cryst. Growth* **134** 353
[6] Ginibre M, Akamatsu S and Faivre G 1997 *Phys. Rev. E* **56** 780
[7] Akamatsu S, Bottin-Rousseau S, Şerefoğlu M and Faivre G 2012 *Acta Mater.* **60** 3206
[8] Zhu Y C, Wang J C, Yang G C and Zhao D W 2007 *Chin. Phys.* **16** 805
[9] Akamatsu S, Faivre G and Ihle T 1995 *Phys. Rev. E* **51** 4751
[10] Okada T and Saito Y 1996 *Phys. Rev. E* **54** 650
[11] Akamatsu S and Ihle T 1997 *Phys. Rev. E* **56** 4479
[12] Song Y, Akamatsu S, Bottin-Rousseau S and Karma A 2018 *Phys. Rev. Mater.* **2** 053403
[13] Guo C, Li J J, Yu H L, Wang Z J, Lin X and Wang J C 2017 *Acta Mater.* **136** 148
[14] Li J J, Wang Z J, Wang Y Q and Wang J C 2012 *Acta Mater.* **60** 1478
[15] Karma A 1987 *Phys. Rev. Lett.* **59** 71
[16] Coullet P, Goldstein R E and Gunaratne G H 1989 *Phys. Rev. Lett.* **63** 1954
[17] Faivre G, Cheveigne S de, Guthmann C and Kurowski P 1989 *Europhys. Lett.* **9** 779
[18] Kassner K and Misbah C 1991 *Phys. Rev. A* **44** 6513

[19] Kassner K and Misbah C 1991 *Phys. Rev. A* **44** 6533
[20] Kassner K and Misbah C 1992 *Phys. Rev. A* **45** 7372
[21] Kassner K and Misbah C 1992 *J. Phys. A: Math. Gen.* **25** 3213
[22] Akamatsu S, Plapp M, Faivre G and Karma A 2002 *Phys. Rev. E* **66** 030501
[23] Akamatsu S, Faivre G, Plapp M and Karma A 2004 *Metall. Mat. Trans. A* **35** 1815
[24] Jackson K A and Hunt J D 1988 *Dynamics of Curved Fronts* (New York: Academic Press) pp. 363–376
[25] Caroli B, Caroli C, Faivre G and Mergy J 1992 *J. Cryst. Growth* **118** 135
[26] Akamatsu S, Bottin-Rousseau S, Şerefoğlu M and Faivre G 2012 *Acta Mater.* **60** 3199
[27] Bottin-Rousseau S, Şerefoğlu M, Akamatsu S and Faivre G 2012 *IOP Conf. Ser.: Mater. Sci. Eng.* **27** 012088
[28] Bottin-Rousseau S, Medjkoune M, Senninger O, Carroz L, Soucek R, Hecht U and Akamatsu S 2021 *J. Cryst. Growth* **570** 126203
[29] Lahiri A, Tiwary C, Chattopadhyay K and Choudhury A 2017 *Comp. Mater. Sci.* **130** 109
[30] Rátkai L, Tóth G I, Környei L, Pusztai T and Gránásy L 2017 *J. Mater. Sci.* **52** 5544
[31] Hecht U, Eiken J, Akamatsu S and Bottin-Rousseau S 2019 *Acta Mater.* **170** 268
[32] Mohagheghi S, Hecht U, Bottin-Rousseau S, Akamatsu S, Faivre G and Şerefoğlu M 2019 *IOP Conf. Ser.: Mater. Sci. Eng.* **529** 012010
[33] Aramanda S K, Khanna S, Salapaka S K, Chattopadhyay K and Choudhury A 2020 *Metall. Mater. Trans. A* **51** 6387
[34] Aramanda S K, Khanna S, Salapaka S K, Chattopadhyay K and Choudhury A 2020 *Mater. Sci. Eng. A* **51** 6327
[35] Ghosh S and Plapp M 2015 *Trans. Indian Inst. Met.* **68** 1235
[36] Ghosh S and Plapp M 2017 *Acta Mater.* **140** 140
[37] Ghosh S, Choudhury A, Plapp M, Bottin-Rousseau S, Faivre G and Akamatsu S 2015 *Phys. Rev. E* **91** 022407
[38] Tu Z, Zhou J, Zhang Y, Li W and Yu W. 2020 *J. Cryst. Growth* **549** 125851
[39] Tu Z, Zhou J, Tong L and Guo Z 2020 *J. Cryst. Growth* **532** 125439
[40] Kim S G, Kim W T, Suzuki T and Ode M 2004 *J. Cryst. Growth* **261** 135
[41] Hötzer J, Jainta M, Steinmetz P, Nestler B, Dennstedt A, Genau M, Bauer M, Köstler H and Rüde U 2015 *Acta Mater.* **93** 194
[42] Kellner M, Hötzer J, Schoof E and Nestler B 2020 *Acta Mater.* **182** 267
[43] Pusztai T, Rátkai L, Horváth L and Gránásy L 2022 *Acta Mater.* **227** 117678
[44] Kim S G 2007 *Acta Mater.* **55** 4391